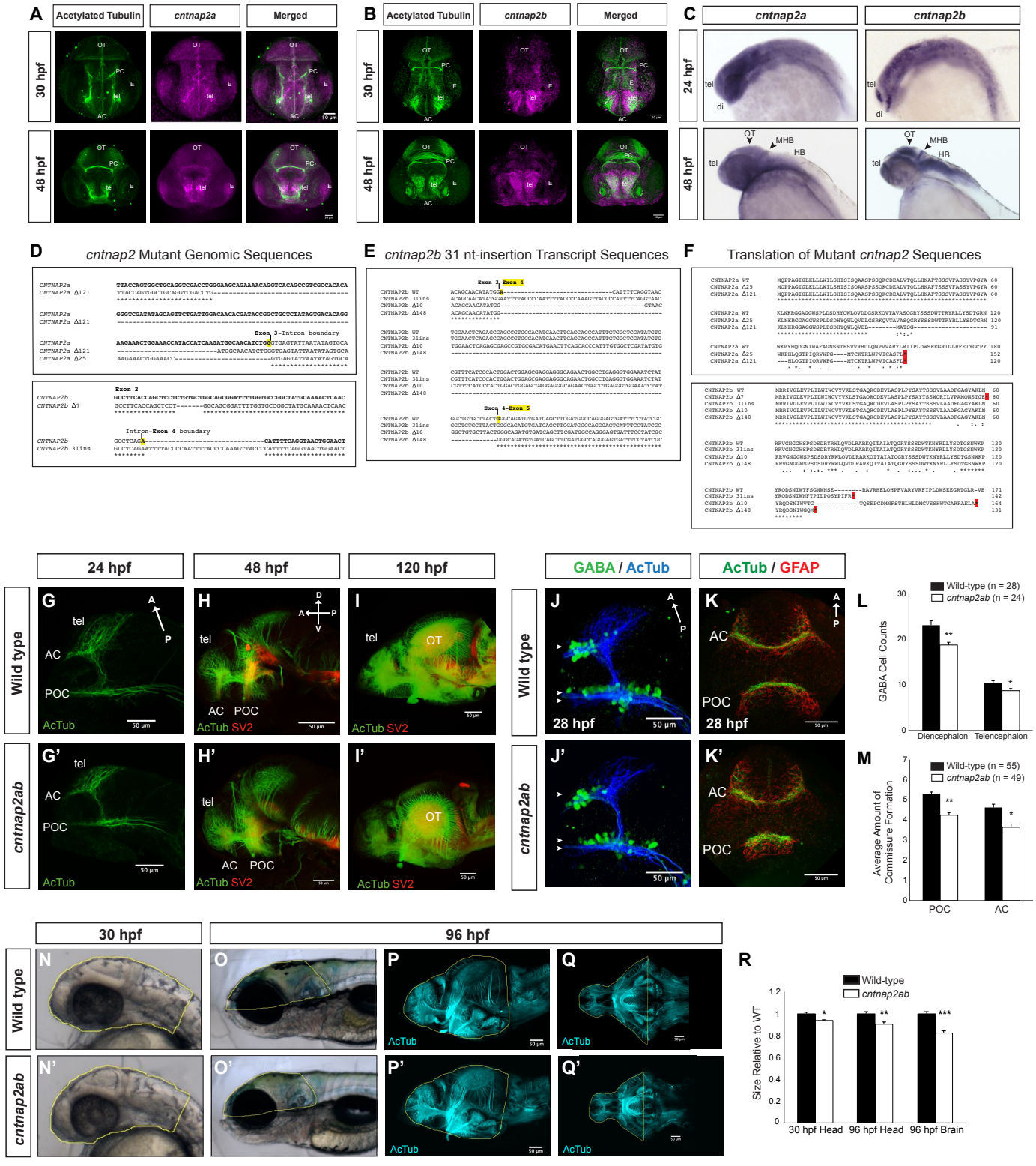

Figure S1, Related to Figure 1. Generation of *cntnap2ab* mutants and characterization of brain structure.

Figure S1, Related to Figure 1. Generation of *cntnap2ab* mutants and characterization of brain structure.

A, B. Fluorescent *in situ* hybridization of *cntnap2a* and *cntnap2b* expression and acetylated tubulin in wild-type embryos at 30 and 48 hpf.

C. Whole mount *in situ* hybridization of *cntnap2a* and *cntnap2b* in wild-type embryos at 24 and 48 hpf. Both paralogs are expressed in the CNS, though *cntnap2b* shows a more specific expression pattern in the telencephalon and diencephalon (24 hpf), the optic tectum, midbrain-hindbrain boundary, and hindbrain (48 hpf).

D. Genomic sequences of insertion-deletion mutations generated by zinc finger nucleases in each *cntnap2* paralog. These include Δ121 and Δ25 in exon 3 of *cntnap2a* (top) and Δ7 in exon 2 and a 31-nt insertion in exon 4 of *cntnap2b* (bottom), all of which produce a frameshift and premature stop codon.

E. Alternatively spliced transcripts resulting from the 31-nt allele in exon 4 of *cntnap2b* identified by RT-PCR of exons 1 to 6 at 5 dpf. These transcripts include: (i) the 31-nt sequence itself, as in the genomic sequence; (ii) Δ10 in exon 4: because the 31-nt insertion occurs close to the intron-exon 4 boundary, an alternate splice site is used (the next "TC*AG*" in the genomic sequence after the actual intronic splice site), which is 10 nt after the beginning of exon 4; (iii) Δ148 due to splicing of the entire exon 4. All 3 transcripts produce a frameshift and a premature stop codon. We did not identify alternatively spliced transcripts resulting from the other mutations in either gene.

F. Sequence alignment of wild type Cntnap2a (top) and Cntnap2b (bottom) proteins and the translation of mutant transcripts. All mutant transcripts are predicted to cause premature stop codons in the discoidin domains of both proteins (Figure 1A).

G-I. Acetylated tubulin (AcTub) and synaptic vesicle protein 2 (SV2) labeling in wild-type (**G-I**) and *cntnap2a*$^{\Delta 121/\Delta 121}$*cntnap2b*$^{31i/31i}$ (**G'-I'**) fish at 24, 48, and 120 hpf. While there is a transient delay in the formation of the anterior and post-optic commissures in *cntnap2ab* mutants at 28 hpf (see **K, K', M**), these commissures form by later stages. Brain structure is not otherwise grossly disrupted in *cntnap2ab* mutants up to 120 hpf.

J-K. Acetylated tubulin and GABA (**J, J'**) or GFAP (glial cells) (**K, K'**) in wild-type and *cntnap2a*$^{\Delta 121/\Delta 121}$*cntnap2b*$^{31i/31i}$ (*cntnap2ab*) mutants at 28 hpf.

L. There are significantly fewer GABA+ cells in both the telencephalon (arrowheads) and diencephalon (double arrowheads) of *cntnap2ab* (**J'**) versus wild-type (**J**) larvae at 28 hpf. GABA+ cells were counted in z-stack images by three blinded raters. (*p=0.00782, telencephalon; **p=0.0181, diencephalon, two-way ANOVA, genotype factor.)

M. The formation of the anterior commissure (AC) and post-optic commissure (POC) is delayed in *cntnap2a*$^{\Delta 121/\Delta 121}$*cntnap2b*$^{31i/31i}$ (*cntnap2ab*) (**K'**) compared to wild-type (**K**) larvae (*p=0.00428, AC; **p=0.0159, POC, two-way ANOVA, genotype factor.) Three blinded raters quantified the degree of commissure formation based on a qualitative rating scale ranging from no axons crossing (1) to complete formation (7), as previously described (Barresi et al., 2005). The POC appears to be less fasciculated in mutants. Glial bridge formation is largely intact.

N-R Head and brain size in wild-type (**N-Q**) and *cntnap2a*$^{\Delta 121/\Delta 121}$*cntnap2b*$^{31i/31i}$ (*cntnap2ab*) (**N'-Q'**). Representative tracings done in Fiji are shown in yellow. The posterior boundaries of the head and brain were defined by the otic vesicle and the midbrain-hindbrain boundary, respectively.

R. *cntnap2ab* mutant heads are 6.5% and 9.7% smaller than wild-type at 30 hpf and 96 hpf, respectively, and mutant brains are 18% smaller than wild-type at 96 hpf. (*p=9.71x10^{-7}, 30 hpf head size; **p=0.00513, 96 hpf head size; ***p=3.89x10^{-6}, 96 hpf brain size; one-way ANOVA). In addition, eye and yolk size measurements indicate that mutant fish are smaller overall (Table S1).

(A, B): frontal views; (C, N-O, N'-O'): lateral views; (G-J, G'-J', P-P'): lateral views of dissected embryos with the eye removed; (K-K'): frontal views of the forebrain; (Q-Q'): ventral views; tel, telencephalon; di, diencephalon; OT, optic tectum; PC, posterior commissure; AC, anterior commissure; POC, post-optic commissure; E, eye; MHB, midbrain-hindbrain boundary; HB, hindbrain.

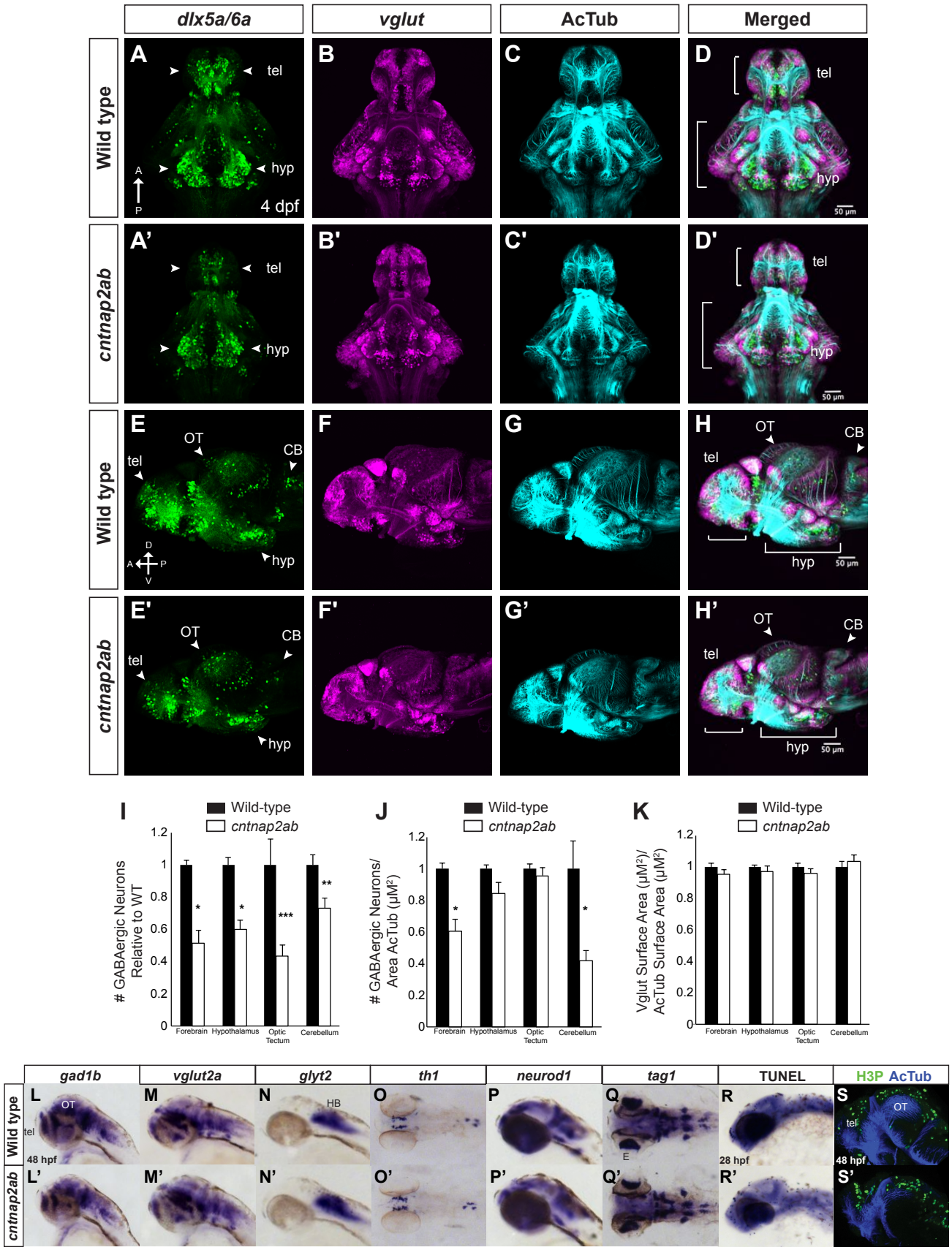

Figure S2, Related to Figure 1. Inhibitory and excitatory neurons in *cntnap2ab* mutants.

Figure S2, Related to Figure 1. Inhibitory and excitatory neurons in *cntnap2ab* mutants.

Immunostainings of reporter gene expression in Tg(*dlx6a-1.4kbdlx5a/dlx6a:GFP*) and Tg(*vglut:DsRed*) in wild-type (**A-H**) and *cntnap2a*$^{\Delta 121/\Delta 121}$*cntnap2b*$^{31i/31i}$ (**A'-H'**) larvae at 4 dpf. **(A-A', E-E'):** The deficit in GABAergic neurons and precursors (*dlx5a6a:*GFP+ cells) is evident in the ventral and dorsal telencephalon (tel), hypothalamus (hyp), and cerebellum (CB) (arrowheads in **A-A'**, **E-E'**). The reduction in GABAergic neurons by surface area of acetylated tubulin is significant in the forebrain and cerebellum (**J**).

I-K. *dlx5a6a:*GFP+ cells, *vglut:*DsRed and acetylated tubulin stainings were quantified by brain region at 4 dpf: forebrain (small brackets in **D-D', H-H'**); hypothalamus (large brackets in **D-D', H-H'**); cerebellum (arrowheads in **E-E', H-H'**); and optic tectum (arrowheads in **E-E', H-H')**. (forebrain and hypothalamus: wild-type, n=9; *cntnap2ab*, n=9; optic tectum and cerebellum: wild-type, n=7; *cntnap2ab*, n=8)

I. *dlx5a6a:*GFP+ cell number normalized to wild-type. (*p<0.001; **p<0.01; ***p<0.02; one-way ANOVA, Bonferroni corrected).

J. *dlx5a6a:*GFP+ cell number relative to acetylated tubulin surface area normalized to wild-type. Because there are significant reductions in GABAergic neurons relative to area in the forebrain and cerebellum, we concluded that the GABAergic deficits in these regions are not primarily attributable to the reduction in brain size. (*p<0.02; one-way ANOVA, Bonferroni corrected).

K. *vglut:*DsRed surface area relative to acetylated tubulin surface area normalized to wild-type. Unlike GABAergic neurons, there are no significant reductions in glutamatergic surface area relative to acetylated tubulin surface area across regions, suggesting these differences are due to the overall reduction in brain size as opposed to regional deficits (p=0.225, forebrain; p=0.444, hypothalamus; p=0.408, optic tectum; p=0.490, cerebellum; one-way ANOVA).

L-S. Analysis of the CNS of wild-type (**L-S**) and *cntnap2a*$^{\Delta 121/\Delta 121}$*cntnap2b*$^{31i/31i}$ (*cntnap2ab*) (**L'-S'**) by *in situ* hybridization at 48 hpf: (**L, L'**): *glutamate decarboxylase 1b* (*gad1b*); (**M**, **M'**): *vesicular glutamate transporter* or *solute carrier family 17, member 6b* (*vglut2a* or *slc17a6b*); (**N**, **N'**): *solute carrier family 6 (neurotransmitter transporter, glycine), member 5* (*glyt2* or *slc6a5*); (**O**, **O'**): *tyrosine hydroxylase* (*th1* or *th*); (**P**, **P'**): *neuronal differentiation 1* (*neurod* or *neurod1*); (**Q**, **Q'**); *transiently expressed axonal glycoprotein* (*tag1*) or *contactin 2* (*cntn2*); **(R, R')**: TUNEL staining at 28 hpf; (**S**, **S'**): phospho-histone H3 (H3P) (green) and acetylated tubulin (blue) immunostaining at 48 hpf. We observed that expression of *gad1b* was variable. No gross differences in the other neurotransmitter systems, markers of neuronal differentiation, apoptosis, or cell proliferation were observed.

(A-D, A'-D', E-H, E'-H') show all channels for the images in Figure 1C-F and 1C'-F', respectively. (A-D, A'-D'): ventral views; (E-H, E'-H', L-N, L'-N'; P-P', R-R', S-S'): lateral views; (O-O', Q-Q'): dorsal views. (tel, telencephalon; hyp, hypothalamus; OT, optic tectum; CB: cerebellum; HB, hindbrain; E, eye.)

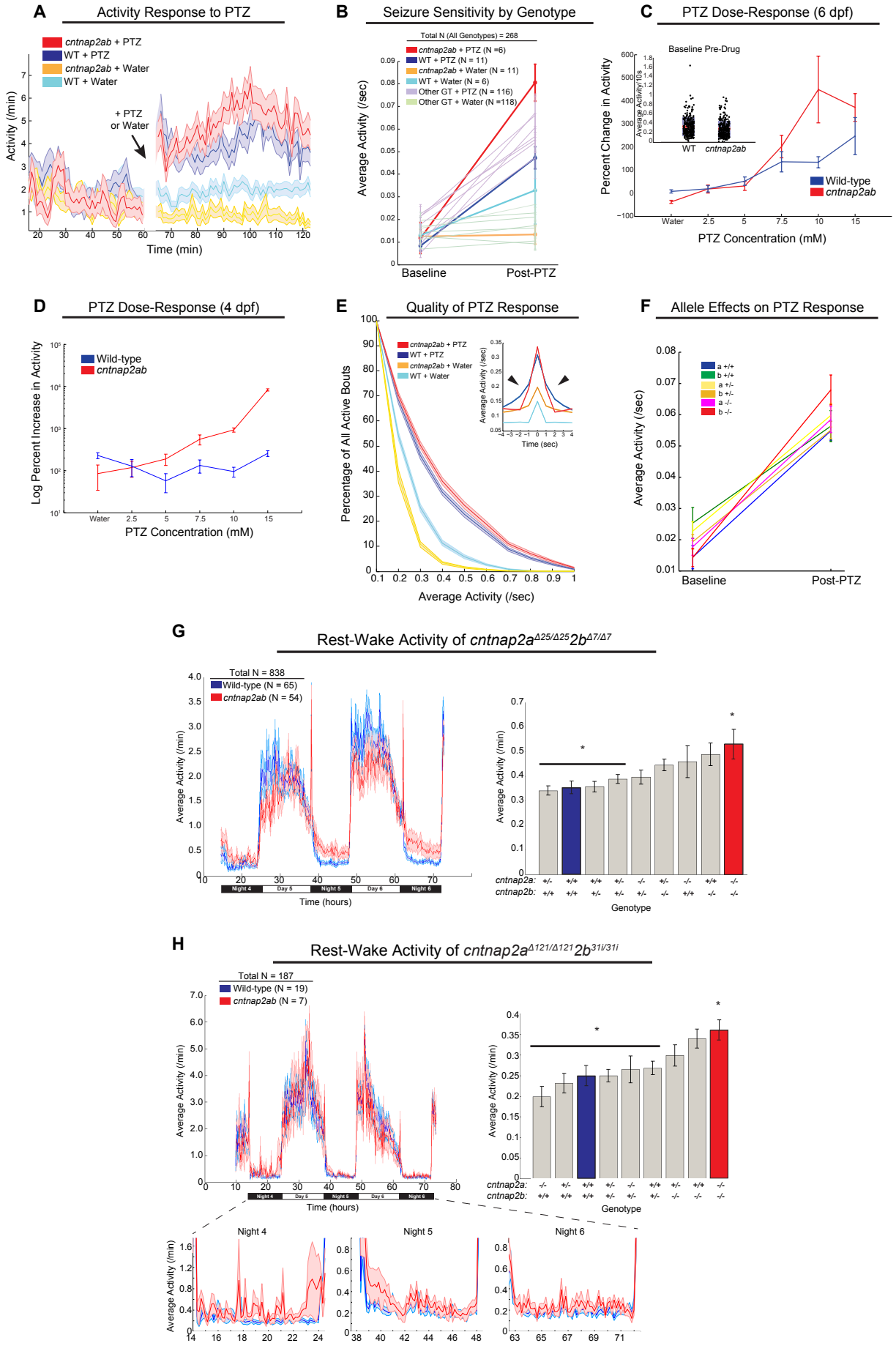

Figure S3, Related to Figures 1 and 2. Drug induced seizure sensitivity and nighttime hyperactivity in *cntnap2ab* mutants.

Figure S3, Related to Figures 1 and 2. Drug-induced seizure sensitivity and nighttime hyperactivity in *cntnap2ab* mutants.

A. Activity tracings of wild-type (WT) and *cntnap2a*$^{\Delta 121/\Delta 121}$*cntnap2b*$^{31i/31i}$ (*cntnap2ab*) larvae at 6 dpf before and after exposure to 10 mM PTZ or water (ribbon shows +/- SEM).

B. Average activity 1 h before and after the blind addition of 10 mM PTZ or water to the progeny of incrosses of *cntnap2a*$^{\Delta 25/+}$*cntnap2b*$^{\Delta 7/+}$ fish, as in Figure 1H, with intermediate genotypes shown. Note that c*ntnap2a*$^{\Delta 25/\Delta 25}$*cntnap2b*$^{\Delta 7/\Delta 7}$ larvae show the greatest PTZ response (p=0.0013, two-way ANOVA, genotype x dose interaction).

C. Dose-response curve showing the percent increase in activity over baseline per fish of wild-type or *cntnap2a*$^{\Delta 121/\Delta 121}$*cntnap2b*$^{31i/31i}$ larvae at 6 dpf exposed to water or increasing concentrations of PTZ for 1 h (p=0.0004, two-way ANOVA, genotype x dose interaction). Inset shows that the average baseline activity for 1 h prior to the addition of water or PTZ is not significantly different in wild-type and *cntnap2ab* larvae.

D. Dose-response curve of the log of the percent increase in activity over baseline per fish for wild-type and *cntnap2a*$^{\Delta 121/\Delta 121}$*cntnap2b*$^{31i/31i}$ larvae at 4 dpf exposed to water or increasing concentrations of PTZ for 1 h. Compared to larvae at 6 dpf (**C**), baseline activity at 4 dpf is relatively low, such that the PTZ response (normalized to baseline) appears greater. Increased PTZ sensitivity in mutants is evident at 4 dpf as well ($p<10^{-6}$, two-way ANOVA, genotype x dose interaction). *cntnap2ab* mutants decrease their activity in response to water, in contrast to wild-type fish, in which water is mildly activating. We hypothesize this difference may reflect deficits in the ability of *cntnap2ab* mutants to respond to mildly stressful stimuli. Given this observation, normalization in the dose-response experiments was done to baseline, pre-PTZ activity per fish.

E. Cumulative histogram showing the percent of all activity in the blinded experiment that occurred 1 h after the addition of PTZ or water (ribbon shows +/- SEM). Most (>90%) baseline activity of 4 dpf larvae is ≤0.3/sec, though PTZ induces robust increases in activity. *cntnap2ab* mutants are more likely than background-matched wild-type larvae to have activity bouts 0.5/sec in response to PTZ. Inset shows the average activity (± SEM) centered on all locomotor events that occurred within 1 h of the addition of PTZ or water. Note that PTZ-induced activity bouts occur more sparsely in mutants compared to wild-type, as evidenced by the decreased likelihood of a bout to be immediately preceded or followed by another bout (arrowheads).

F. Plot of average activity by *cntnap2* allele before and after the blind addition of 10 mM PTZ or water at 6 dpf. This graph highlights that increased sensitivity to PTZ is primarily driven by the *cntnap2b* allele (p=0.5703, a allele x drug interaction; p=0.0046, b allele x drug interaction; p=0.10, a allele versus b allele interaction, two-way ANOVA).

G. Rest-wake locomotor activity of *cntnap2a*$^{\Delta 25/\Delta 25}$*cntnap2b*$^{\Delta 7/\Delta 7}$ (*cntnap2ab,* red) and wild-type (blue) sibling-matched larvae over 72 h, as in Figure 2B. The bar graph shows the average locomotor activity of wild-type, *cntnap2a*$^{\Delta 25/\Delta 25}$*cntnap2b*$^{\Delta 7/\Delta 7}$ and all intermediate genotypes on all nights. We observed a general trend in strengthening of the phenotype with a reduction in *cntnap2ab* gene dosage (see also Figure S3H). (*$p=1.2x10^{-4}$, one-way ANOVA followed by Tukey's post-hoc testing shows the differences lie between the double homozygous larvae and the genotypes marked with the black bar.)

H. Locomotor activity of *cntnap2a*$^{\Delta 121/\Delta 121}$*cntnap2b*$^{31i/31i}$ (*cntnap2ab*, red) and wild-type (blue) background-matched larvae over 72 h. In total, 187 larvae were tracked blind to genotype. Magnified graphs of activity on each night are shown. The bar graph shows average locomotor activity of wild-type, *cntnap2a*$^{\Delta 121/\Delta 121}$*cntnap2b*$^{31i/31i}$ and all intermediate genotypes on all nights. Note that double homozygous mutants demonstrate the greatest level of activity, though single homozygotes for the *cntnap2b* mutation (*cntnap2a*$^{+/+}$*cntnap2b*$^{31i/31i}$ or *cntnap2a*$^{+/-}$ *cntnap2b*$^{31i/31i}$ larvae) are hyperactive as well, indicating the *cntnap2b* allele may be driving the hyperactivity phenotype in this line (*p=0.0198, all nights, one-way ANOVA followed by Tukey's post-hoc testing shows the differences lie between the double homozygous larvae and the genotypes marked with the black bar.) The difference in the relative allelic effects in the two mutant lines may be due to background variation that influences allelic expression, the smaller dataset for the *cntnap2a*$^{\Delta 121/\Delta 121}$*cntnap2b*$^{31i/31i}$ line, or the nature of the mutations themselves, i.e. alternatively spliced transcripts. However, the effect of total disruption of Cntnap2 on nighttime activity in double homozygotes is robust and consistent in both mutant lines.

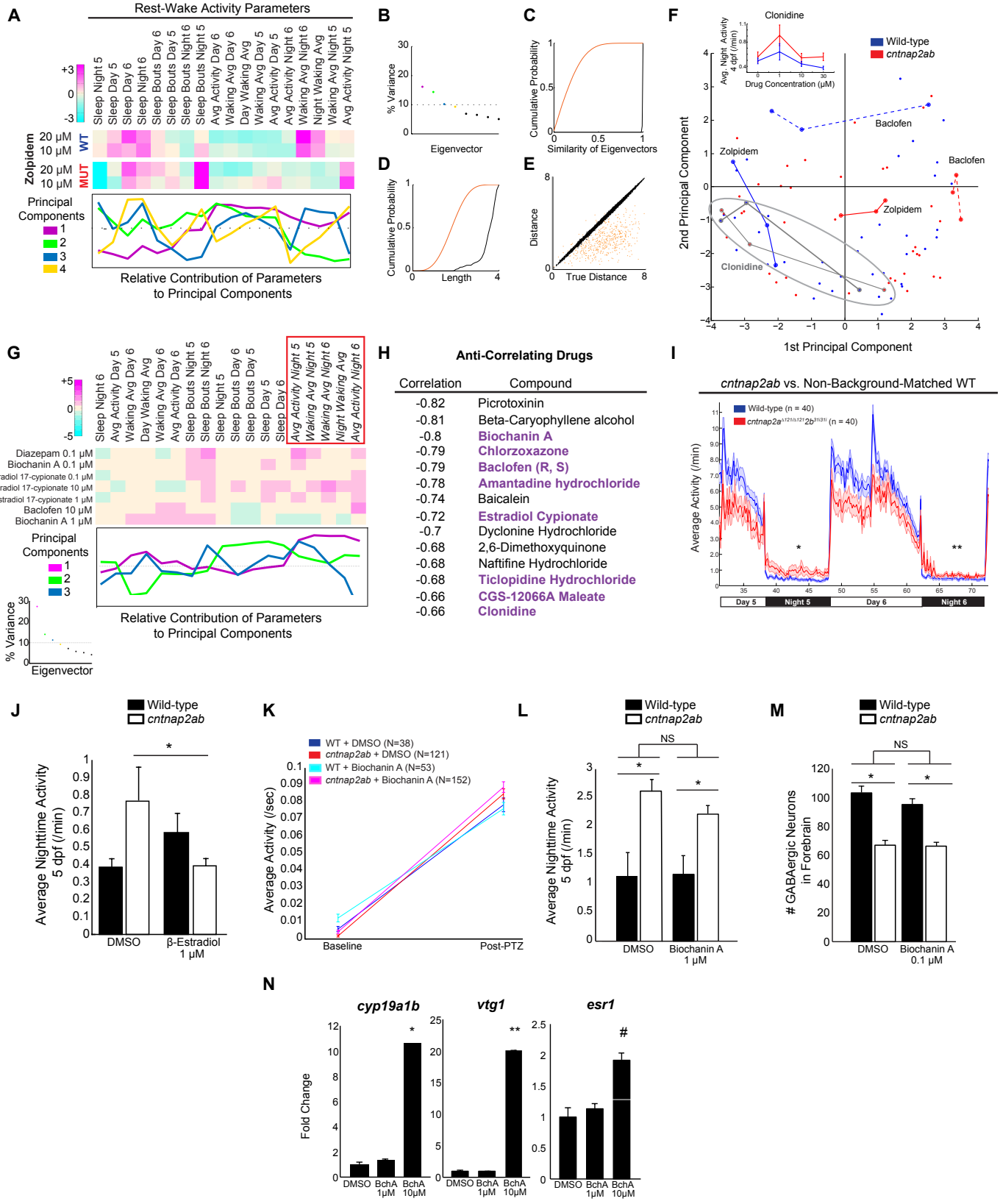

Figure S4, Related to Figures 3 and 4. Differential pharmacological responses of *cntnap2ab* mutants and suppression of nighttime hyperactivity by estrogenic compounds.

Figure S4, Related to Figures 3 and 4. Differential pharmacological responses of *cntnap2ab* mutants and suppression of nighttime hyperactivity by estrogenic compounds.

A. Magnified sections of the clustergram of the behavioral profiles of wild-type (WT) or *cntnap2a*$^{\Delta 12 1/\Delta 12 1}$*cntnap2b*$^{31i/31i}$ (MUT) larvae exposed to 14 psychoactive agents (as in Figure 3F) show differential responses to zolpidem (10 μM, 20 μM). Each rectangle in the clustergram represents the Z-score relative to the behavior of wild-type or *cntnap2a*$^{\Delta 12 1/\Delta 12 1}$*cntnap2b*$^{31i/31i}$ larvae exposed to DMSO alone (magenta, higher than DMSO; cyan, lower than DMSO). The eigenvectors for the first four PCA components are plotted below the clustergram to show the relative contribution of the 18 rest-wake cycle parameters (above) to each PCA component. Compared to the 26 rest-wake parameters, as shown in Figure 2E, in subsequent hierarchical clustering and PCA analyses (Figures 3F and 4B), the length and latency parameters were removed, because these parameters are non-normally distributed across drug-exposed samples, thereby skewing the PCA analysis.

B. Scree plot showing the percentage of the variance that is explained by each principal component in the PCA. Note that four components explain ~50% of the variance. The first four components are shown in magenta, green, blue, and yellow, respectively, corresponding to the components plotted in **(A)**.

C-E. To confirm the stability of the PCA, we asked how the distribution of eigenvectors would change if each drug-dose combination was removed sequentially from the dataset, following the method of (Woods et al., 2014). We applied this "left-out" modeling approach to our dataset (black) and to a randomized permutation of our dataset (orange).

C. Plot of the cumulative probability versus the similarity of eigenvectors for the "left-out" models of our dataset (black) and the randomized dataset (orange). The eigenvectors remain more similar in our model compared to the randomized dataset.

D. Plot of cumulative probability versus length in the "left-out" models shows that the distance from the origin of eigenvectors in our dataset (black) is greater compared to the randomized dataset (orange).

E. Comparison of the distances between vectors for each drug-dose combination in the "left-out" model of our dataset (black dots) versus the randomized set (orange dots). Observe that in our model, the spatial distance between eigenvectors is relatively maintained, unlike in the randomized dataset.

F. Wild-type (blue) and *cntnap2a*$^{\Delta 12 1/\Delta 12 1}$*cntnap2b*$^{31i/31i}$ (*cntnap2ab*, red) behavioral responses to the three doses of zolpidem (solid lines) and (±)-baclofen (dashed lines) can be represented by plotting the first two components of the PCA. Note the distinct location and shape of the wild-type and mutant plots, indicating that these drugs induce differential responses, as shown quantitatively for zolpidem in Figure 3C. In contrast, plots of the first two components of the PCA showing the behavioral responses to three doses of clonidine (gray) in wild-type (thick line, blue dots) and *cntnap2ab* (thin line, red dots) are shown. Note that the location and shape of the mutant and wild-type curves is similar for clonidine, which indicates that this drug has a similar behavioral effect in wild-type and mutant larvae, unlike zolpidem and baclofen. The unlabeled dots represent the responses of wild-type (blue) and *cntnap2ab* (red) larvae to other drugs in PCA space. A representative plot of average night activity at 4 dpf for clonidine (inset) shows that clonidine induces similar dose-dependent behavioral effects on nighttime activity at 4 dpf in wild-type (blue) and *cntnap2ab* (red) larvae ($p=0.744$, two-way ANOVA, genotype x drug interaction).

G. Magnified section of the clustergram in Figure 4B. Observe that biochanin A (0.1 μM, 1 μM) and three doses of β-estradiol 17-cypionate (0.1, 1, and 10 μM) are in this cluster, which highlights the drugs that induce the strongest phenotypic suppression. Each rectangle in the clustergram represents the Z-score of mutants relative to wild-type + no drug (cream color = wild-type level; magenta, higher than wild-type; cyan, lower than wild-type). The eigenvectors for the first three PCA components are plotted below the clustergram to show the relative contribution of the rest-wake cycle parameters (above) to each PCA component, as in **(A).** The red box highlights the parameters that measure nighttime activity. Scree plot (lower left inset) shows that three components explain ~50% of the variance. These components are shown in magenta, green, and blue, respectively, corresponding to the components plotted on the graph. The stability of the PCA was confirmed using the "left-out" model (Woods et al., 2014), as in **(B-E)** (data not shown). Of note, we found that the lowest dose of risperidone (0.001 μM) reverses nighttime hyperactivity in *cntnap2ab* mutants, yet based on the PCA, it appears to rescue with less phenotypic selectivity than biochanin A (Figure 4C, D, F), suggesting that its effect on nighttime hyperactivity is less phenotypically specific.

At the same time, the effects of risperidone appear to be highly dose-dependent, suggesting that it may affect various pharmacological pathways at different dose ranges. Further experiments are needed to investigate the differential responses of wild-type and mutant larvae to risperidone across a range of doses.

H. The top anti-correlating psychoactive agents and their degree of anti-correlation relative to the *cntnap2a*$^{\Delta 25/\Delta 25}$*cntnap2b*$^{\Delta 7/\Delta 7}$ mutant behavioral profile. Drugs shown in bold purple letters were selected for further testing in wild-type and mutant fish (Figure 3A). It is possible that other agents on this list in addition to biochanin A may have the ability to suppress the mutant behavioral phenotype. It will be interesting in future studies not only to test all of the anti-correlating small molecules, but to test all 550 psychoactive agents in *cntnap2ab* and other zebrafish mutants of ASD genes, which will provide substantial leverage to investigate convergent biological mechanisms among ASD risk genes.

I. Locomotor activity of *cntnap2a*$^{\Delta 121/\Delta 121}$*cntnap2b*$^{31i/31i}$ (red) and wild-type (blue) non-background-matched larvae over 72 hours (n=40 per group). *cntnap2ab* mutants display nighttime hyperactivity relative to unrelated wild-type (*night 5, p=0.0079; **night 6, p=0.022; one-way ANOVA), consistent with our findings in background-matched larvae. Mutants also show significantly less daytime activity relative to unrelated wild-type controls (p=0.005, one-way ANOVA). Because this effect did not reach statistical significance in sibling-matched control experiments (Table S2), we concluded that this difference is likely due to background or environmental variation.

J. Effect of β-estradiol (1 μM) on average night waking activity at 5 dpf in wild-type and *cntnap2a*$^{\Delta 121/\Delta 121}$*cntnap2b*$^{31i/31i}$ larvae (*p=0.017, two-way ANOVA, genotype x drug interaction).

K. To assess the extent to which biochanin A reverses PTZ-induced seizures, wild-type and *cntnap2a*$^{\Delta 121/\Delta 121}$*cntnap2b*$^{31i/31i}$ mutants were exposed daily and chronically to biochanin A (1 μM) or DMSO from 24 hpf to 4 dpf, and then exposed to PTZ in the presence of biochanin A or DMSO. Exposure to biochanin A did not rescue the increased sensitivity of *cntnap2ab* mutants to PTZ (p=0.237, three-way ANOVA, genotype x drug exposure x PTZ interaction). *cntnap2ab* mutants demonstrated increased sensitivity to PTZ irrespective of biochanin A exposure ($p=3.57\times10^{-4}$, genotype x PTZ exposure).

L. To assess the extent to which long-term exposure to biochanin A reverses nighttime hyperactivity, wild-type and *cntnap2a*$^{\Delta 121/\Delta 121}$*cntnap2b*$^{31i/31i}$ (*cntnap2ab*) embryos were exposed daily to biochanin A (1 μM) or DMSO alone beginning at 24 hpf. After removal of the drug solution at 4 dpf, the locomotor activity of wild-type and *cntnap2ab* larvae was quantified for 48 hours using the automated tracking assay. Exposure to biochanin A followed by washout did not rescue nighttime hyperactivity (*$p=5.51\times10^{-5}$, two-way ANOVA, genotype factor; p=0.454, two-way ANOVA, genotype x drug interaction).

M. To determine whether early exposure to biochanin A reverses the GABAergic deficits in *cntnap2ab* mutants, wild-type and *cntnap2a*$^{\Delta 121/\Delta 121}$*cntnap2b*$^{31i/31i}$ (*cntnap2ab*) embryos were raised in the presence of biochanin A (0.1 μM) or DMSO, which was added at 30 hpf. Immunostainings of reporter gene expression using the transgenic line, Tg(*dlx6a-1.4kbdlx5a/dlx6a:GFP*), were performed and *dlx5a/6a:*GFP+ cells in the forebrain of wild-type and *cntnap2ab* mutants at 4 dpf were counted manually. There are significantly fewer GABAergic neurons in the forebrains of *cntnap2ab* mutants compared to wild-type larvae at 4 dpf irrespective of exposure status (*$p=6.03\times10^{-13}$, two-way ANOVA, genotype factor). Early exposure to biochanin A did not alter the number of GABAergic neurons in *cntnap2ab* or wild-type fish (p=0.190, two-way ANOVA, genotype x drug interaction; wild-type + DMSO, n=13; wild-type + biochanin A, n=17; *cntnap2ab* + DMSO, n=14; *cntnap2ab* + biochanin A, n=15).

N. To ascertain the extent to which biochanin A (BchA) upregulates estrogen response genes, expression of three known estrogen target genes (*cytochrome P450, family 19, subfamily A, polypeptide 1* (*aromatase B, cyp19a1b*); *vitellogenin 1* (*vtg1*); and *estrogen receptor 1* (*esr1*)) (Hao et al., 2013) was measured by qPCR in total RNA extracts from wild-type larvae exposed overnight to biochanin A (1 μM, 10 μM) or DMSO from 4 to 5 dpf. Fold change in gene expression is shown. Note that biochanin A (10 μM) significantly activates estrogen response genes, while the rescue dose (1 μM) has only a weak effect (*p=0.001; **p=0.002; $^{\#}$p=0.1; Dunnett's test).

Table S1, Related to Figure 1. Head and Brain Size Measurements in Wild-type and *cntnap2a*$^{\Delta 121/\Delta 121}$*cntnap2b*$^{31i/31i}$ Mutants at 30 and 96 hpf.

Age	Head Size (Rel. to WT) (± SEM)	p	Eye Size (Rel. to WT) (± SEM)	p	Yolk Size (Rel. to WT) (± SEM)	p
30 hpf	0.935 ± 0.00783	9.71×10^{-7}	0.851 ± 0.0190	1.50×10^{-6}	0.902 ± 0.00613	0.00132
96 hpf	0.903 ± 0.0236	0.00513	0.873 ± 0.0198	0.00106	N/A	N/A
96 hpf brain	0.820 ± 0.0226	3.89×10^{-6}	N/A	N/A	N/A	N/A

Age	Head:Eye Ratio			Head:Yolk Ratio		
	WT	Mutant	p	WT	Mutant	p
30 hpf	4.80 ± 0.0679	5.33 ± 0.112	0.00082	0.574 ± 0.00672	0.595 ± 0.0068	0.11
96 hpf	2.14 ± 0.0549	2.21 ± 0.0795	0.458	N/A	N/A	N/A

At 30 hpf: WT, n=22; Mutant, n=24; 96 hpf: WT, n=9; Mutant, n=7; 96 hpf brains WT, n=11, Mutant, n=14.
For yolk size measurements at 30 hpf: WT, n=21; Mutant n=23.

Table S2, Related to Figure 2. Rest-wake Cycle Parameters in Background-Matched Wild-type and *cntnap2a*$^{\Delta 25/\Delta 25}$*cntnap2b*$^{\Delta 7/\Delta 7}$ Larvae at 4-6 dpf.

Time	Wild-type	*cntnap2ab*	p	Wild-type	*cntnap2ab*	p	Wild-type	*cntnap2ab*	p
	Total Sleep (minutes)			**Number of Sleep Bouts**			**Sleep Bout Length (minutes)**		
Night 4	453 ± 11.1	414 ± 16.7	**0.0451**	59.8 ± 3.57	64.0 ± 3.76	0.4143	11.0 ± 1.07	8.47 ± 0.853	0.0793
Night 5	362 ± 16.0	324 ± 21.0	0.1459	76.9 ± 3.44	75.4 ± 4.08	0.7826	6.28 ± 0.709	5.94 ± 0.945	0.7714
Night 6	342 ± 15.9	309 ± 19.6	0.194	81.1 ± 3.45	81.8 ± 4.29	0.8973	6.09 ± 0.939	5.53 ± 1.04	0.6904
Day 5	351 ± 29.3	417 ± 34.8	0.1448	66.3 ± 5.44	59.5 ± 4.09	0.3132	6.85 ± 0.759	7.12 ± 0.779	0.8068
Day 6	234 ± 26.8	283 ± 32.2	0.2459	59.9 ± 4.70	73.0 ± 7.15	0.1159	4.01 ± 0.697	4.51 ± 0.714	0.6186
	Sleep Latency (minutes)			**Average Activity (seconds/minute)**			**Waking Activity (seconds/minute)**		
Night 4	17.0 ± 0.493	21.1 ± 3.73	0.2264	0.281 ± 0.0315	0.440 ± 0.0783	**0.0478**	0.916 ± 0.0588	1.00 ± 0.0880	0.4103
Night 5	12.0 ± 1.61	10.3 ± 0.902	0.372	0.363 ± 0.0342	0.596 ± 0.103	**0.0234**	0.767 ± 0.059	0.969 ± 0.104	0.0825
Night 6	7.46 ± 0.820	9.81 ± 1.22	0.1025	0.349 ± 0.0257	0.649 ± 0.139	**0.0222**	0.659 ± 0.0310	0.940 ± 0.144	**0.0394**
Day 5	3.60 ± 1.14	4.69 ± 1.58	0.5695	1.88 ± 0.177	1.57 ± 0.212	0.2615	2.89 ± 0.189	2.47 ± 0.212	0.137
Day 6	13.2 ± 7.86	7.07 ± 2.13	0.4878	2.42 ± 0.190	2.037 ± 0.215	0.1817	3.19 ± 0.209	2.72 ± 0.253	0.1462

Table S3, Related to Figure 2. Acoustic Startle, Habituation, and Optokinetic Response Assays in Wild-type and *cntnap2a*$^{\Delta 121/\Delta 121}$*cntnap2b*$^{31i/31i}$ Larvae at 5-7 dpf.*

Acoustic Startle and Habituation

	Short Latency C-bend (SLC)[a] Sensitivity (% Response)		Long Latency C-bend (LLC)[a] (% Response)		SLC Habituation	Prepulse Inhibition
Genotype	13 dB	26 dB	13 dB	19.8 dB	Average (%)	Average (%)
Wild-type	7.5 ± 2.45	83.7 ± 4.27	22.9 ± 3.36	37.2 ± 4.1[b]	96.2 ± 1.07	64.0 ± 3.35
cntnap2a$^{\Delta 121/+}$*2b*$^{31i/+}$	10.6 ± 1.22	86.9 ± 1.87	23.6 ± 2.16	34.1 ± 2.23[c]	95.5 ± 1.12	60.0 ± 3.09
cntnap2a$^{\Delta 121/\Delta 121}$ *2b*$^{31i/31i}$	8.89 ± 2.41	89.4 ± 3.92	15.6 ± 5.00	22.6 ± 4.62[b,c]	97.4 ± 0.97	62.3 ± 3.66

[a]Tested in background-matched controls. [b]*p = 0.025,* [c]*p =0.039, t-test*

Optokinetic Response

Genotype	% contrast (# saccades/min ± SEM)						Spontaneous Saccades
	100	70	40	20	10	5	
Wild-type	10.3 ± 0.52[d]	10.3 ± 0.67	8.04 ±0.51	6.99 ± 0.45	6.34 ± 0.52	5.9 ± 0.52	5.59 ± 0.45
cntnap2a$^{\Delta 121/+}$*2b*$^{31i/+}$	10.4 ± 0.49[e]	9.59 ± 0.61	8.07 ± 0.46	6.84 ± 0.55	5.87 ± 0.43	5.69 ± 0.36	4.95 ± 0.50
cntnap2a$^{\Delta 121/\Delta 121}$ *2b*$^{31i/31i}$	8.74 ± 0.47[d, e]	8.72 ± 0.43	6.49 ± 0.53	5.60 ± 0.53	5.15 ± 0.49	4.84 ± 0.44	5.67 ± 0.42

[d]*p = 0.04,* [e]*p =0.036, t-test*

*While there were no significant differences in acoustic startle, habituation, or pre-pulse inhibition (PPI) in *cntnap2a*$^{\Delta 121/\Delta 121}$*cntnap2b*$^{31i/31i}$ fish at 5 to 7 dpf, mutants were significantly less likely to perform long-latency "C-bends" (LLC) in response to a 19.8 dB acoustic stimulus. LLC responses are kinematically distinct from short-latency C-bend startle responses (SLC) and have different genetic and neural circuit requirements than SLC responses. While the specific neurons required for LLC behavior are not well understood, LLC-like responses may be involved in coordinated escape movements in schooling fish (Burgess and Granato, 2007). In addition, we did not detect differences in spontaneous saccadic eye movements or OKR performance at most contrast sensitivities in *cntnap2ab* mutants at 5 to 7 dpf, though at the highest contrast level (100%), mutants displayed significantly lower OKR performance compared to wild-type fish. The absence of robust phenotypes in these larval behavioral assays further supports the specificity of the nighttime hyperactivity phenotype detected in our rest-wake assay. Further studies are indicated to dissect the deficits in circuitry underlying these subtle behavioral differences.

Table S4, Related to Figures 3 and 4. Final concentrations of each psychoactive compound tested in wild-type and *cntnap2a*$^{\Delta 121/\Delta 121}$*cntnap2b*$^{31i/31i}$ larvae.

Compound	Catalog #	Company	Dose Range (μM)
Amantadine hydrochloride	A1260	Sigma	3, 10, 30
(±)-Baclofen	B5399	Sigma	0.1, 1, 10
β-estradiol 17-cypionate	E8004	Sigma	0.1, 1, 10, 30
Biochanin A	D2016	Sigma	0.1, 1, 10
Chlorzoxazone	C4397	Sigma	1, 10, 30
Clonidine hydrochloride	C7897	Sigma	1, 10, 30
CSG-12066 maleate salt	C106	Sigma	0.1, 1, 10
Diazepam C-IV	D0899	Sigma	0.1, 1, 10
β-Estradiol	E1024	Sigma	1, 10, 30
L-701,324	L0258	Sigma	3, 10, 30
(-)-MK-801 hydrogen maleate	M108	Sigma	3, 10, 30
Risperidone	R3475	LKT Laboratories	0.001, 0.01, 1, 10, 30
Ticlopidine hydrochloride	T6654	Sigma	1, 10, 30
Zolpidem	N/A	Gift from David Sugden	1, 10, 20

Supplemental Experimental Procedures

Zinc finger nuclease design

CompoZr custom zinc finger nucleases (ZFN) targeting zebrafish *cntnap2a* and *cntnap2b* were designed by Sigma-Aldrich. CompoZr ZFN contain a DNA-binding domain and an obligate-heterodimer *FokI* nuclease domain, engineered for improved specificity (Miller et al., 2007). Activity of ZFN pairs as determined by the yeast MEL-1 reporter assay (Doyon et al., 2008) was >50% for all pairs (*cntnap2a*, 115.1%; *cntnap2b*, Exon 2, 141.0%; *cntnap2b*, Exon 4: 86.3%). Target sequences for each ZFN pair are shown below. ZFN left and right array binding sites are in capital letters and the cut sites are shown in bold lower case letters.

***cntnap2a,* Exon 3:** AACTGGAAACCAT**accatc**AAGATGGCAACATCTGGG
***cntnap2b*, Exon 2:** AGCGCCTTCACCAGCTCC**tctgtg**CTGGCAGCGGAT
***cntnap2b*, Exon 4:** CTCTTCTTTCTGCCTCAGA**catttt**CAGGTAACTGGAACTCAG

Generation and screening of *cntnap2ab* double mutants

To generate mutants, 25, 50, or 75 pg of each left and right ZFN mRNA directed against either *cntnap2a* or *cntnap2b* was injected into wild-type embryos (F_0) at the one-cell stage. Plasmids encoding ZFN (pZFN) were linearized by XhoI digestion. Capped mRNA was synthesized by *in vitro* transcription and the polyA tail was added using the mMessage mMachine T7 Ultra transcription kit (Ambion) following the manufacturer's protocol. mRNA was purified using the RNeasy Mini Kit (Qiagen). Each ZFN set was screened to determine the optimal concentration that induced somatic mutations at the target site while minimizing toxicity, as previously described (Foley et al., 2009; Sander et al., 2011). In brief, genomic DNA was isolated from 10 injected 24 hpf embryos that were viable and lacked developmental defects, and the ZFN target region was amplified by limited-cycle PCR and cloned using the TOPO-TA kit (Invitrogen). The somatic mutation frequency was determined based on the number of insertion-deletion mutations observed by high-resolution fragment analysis of PCR-amplified plasmid DNA from 100 transformed colonies. The following somatic mutation frequencies were ascertained for each ZFN set: *cntnap2a*: 36%, *cntnap2b*, Exon 2: 70%, *cntnap2b*, Exon 4: 12%. Morphologically normal embryos were raised to adulthood and screened for germline mutations, according to the method described in (Cifuentes et al., 2010), with some modifications. Briefly, to genotype the progeny of intercrossed founders, 32 F_1 embryos were screened in groups of two, which were sorted into the wells of a 96-well plate. 50 µl of 100 mM NaOH was added to each well and the embryos were boiled for 20 minutes at 95°C, producing a crude DNA extract, which was neutralized by the addition of 15 µl of 1 M Tris-HCl, pH 7.4 (Sigma-Aldrich). 2 µl of this DNA extract was used per PCR reaction, and 1 µl of PCR product was diluted in 9 µl of formamide for high-resolution fragment analysis (DNA Analysis Facility at Yale University). Chromatograms were analyzed by GeneMapper software (Applied Biosystems) to identify insertion-deletion mutations. F_0 founders are mosaic and some were found to have multiple germline mutations. F_0 were backcrossed to wild-type fish and F_1 heterozygotes carrying mutations of interest in *cntnap2a* and *cntnap2b* were crossed to generate double heterozygotes (F_2). Germline frequencies for each mutation were the following: *cntnap2a*: Δ121, Δ25: 17%; *cntnap2b*, Exon 2: Δ7, 63%; Exon 4: 31ins, 29%.

Genotyping was performed using the following sets of PCR primers:

***cntnap2a*, Exon 3, 485 bp:** 5' ACCCTTAAAATTGATAAAAGAACACG 3' /
5' GCAGAAAAGGGGCTAAATTAAAA 3'
***cntnap2b*, Exon 2, 388 bp:** 5' TGCGATGTGTATCATATGTTCTTTT 3' /
5' AAAAAGGTAGCTCAAACTGTAATTG 3'
***cntnap2b*, Exon 4, 404 bp:** 5' CCTTGCATAATTAAACTGAAATGCT 3' /
5' TGGTTCTCTTGTTTCATTTGGTC 3'

Sequences of full-length *cntnap2a* and *cntnap2b*

Because annotations of *cntnap2a* and *cntnap2b* were incomplete at the 5' end in earlier assemblies of the zebrafish genome, Rapid Amplification of cDNA Ends (5' RACE) was performed using the GeneRacer kit (Life Technologies) following the manufacturer's protocol. First, total RNA was isolated from 24, 48, 72 and 120 hpf

embryos using TRIzol reagent (Life Technologies) and purified using the RNeasy Mini Kit (Qiagen). mRNA was isolated from pooled RNA from these four stages using oligo(dT) primer (Invitrogen) fixed to streptavidin magnetic beads (New England Biolabs). The following gene-specific 5' RACE reverse primers were used:
cntnap2a: 5' CCCAGATGTTGCCATCTTGATGGTATGG 3'
cntnap2b: 5' CAGTCCAGTGGGATGAAACGCACATA 3'

After determining the sequence of the first exon of each gene by 5'RACE, full-length *cntnap2a* (BamHI-XhoI) and *cntnap2b* (BstBI-XbaI) were cloned into pCS2+ (+/- 3'HA tags) by RT-PCR using pooled cDNA from 24, 48, 72, and 120 hpf embryos (or 72 and 120 hpf only). The full-length sequences of both genes will be submitted to Ensembl. The current annotation of *cntnap2a* in GRCz10 does not include the sequence of the first exon as determined by 5'RACE in our experiments.

To assess for alternate start sites of either transcript, 5'RACE was performed using the following gene-specific reverse primers:
cntnap2a*:* 5' GTGGAGGTGCTGAAGCTGAAGGTCA 3'
cntnap2a, Nested: 5' CTGCTTCAAAGAAACCACCAACATC 3'
cntnap2a, 2nd Nested: 5' CATTTGCCACCATTACGACAATACA 3'
cntnap2b #1*:* 5' GGTGTGTTGAAAGAAGCAGCGTTCC 3'
cntnap2b #1, Nested: 5' CAACCACAACCTGACTCACAGGTAA 3'
cntnap2b #1, 2nd Nested: 5' GTGCAGTTGCGTTCAATACCACA 3'
cntnap2b #2: 5' CACCGCAGACTCGCCTTCCTTTAGT 3'
cntnap2b #2, Nested: 5' TGCAGTCGCATGAGTATCCATTGTA 3'
cntnap2b #2, 2nd Nested: 5' ATAACTGCTACAGTGGCCCGAACAT 3'

For *cntnap2a*, one specific 5'RACE product of ~3kb was identified corresponding to the full-length transcript with the same start site (data not shown). No other specific 5'RACE products were identified. For *cntnap2b*, mispriming of the GeneRacer 5' Nested primer within *cntnap2b* yielded nonspecific products. These results indicated that there were no shorter transcripts or alternate start sites identified.

Regarding current annotations of zebrafish *cntnap2*, the full-length sequence of *cntnap2a* that we cloned by RT-PCR is not annotated completely in GRCz10, in that it does not include the sequence of the first exon as determined by 5'RACE in our experiments. In the Ensembl genome browser (GRCz10), there is one gene on chromosome 24 corresponding to *cntnap2a* (ENSDARG00000058969) that is predicted to have 2 transcripts: ENSDART00000154039 and ENSDART00000155843, both of which have incomplete 5' coding sequences. The function of ENSDART00000155843, which is predicted to yield a product of 190 aa, is unknown and requires further investigation. In Ensembl (GRCz10), there is one gene on chromosome 2 corresponding to *cntnap2b* (ENSDARG00000074558) that is predicted to have 2 transcripts: ENSDART00000108900 (full-length, 1315 aa) and ENSDART00000155125, which is predicted to encode a protein of 566 aa. Our 5'RACE and western blotting experiments would be expected to detect the longer transcript of *cntnap2a* (ENSDART00000154039) and both transcripts of *cntnap2b* (ENSDART00000108900; ENSDART00000155125). No other shorter proteins were detected by western blot using our custom antibody (data not shown), indicating our ZFN-induced mutants containing indels in exons 2 to 4 would be expected to disrupt Cntnap2a and Cntnap2b function.

In situ hybridization

In situ hybridization was performed according to the method previously described (Thisse et al., 1993). After staining, embryos were fixed in 4% PFA, washed in PBST and sequentially dehydrated in methanol. Embryos were cleared in benzyl benzoate/benzyl alcohol for imaging. Fluorescent *in situ* hybridization was adapted from the protocol described in (Julich et al., 2005). Probes were detected with anti-Digoxigenin-POD, Fab fragments (Roche, 1:1000) and TSA Plus Cyanine 3 System (Perkin Elmer). Primary antibody to acetylated tubulin (mouse monoclonal IgG2b, #T7451, Sigma-Aldrich, RRID:AB_609894) was used at 1:500. Following staining, embryos were mounted for confocal imaging in low melting point agarose (0.8-1%).

Probes for *cntnap2a* and *cntnap2b* were amplified from a pooled sample of cDNA from 0, 6, 24, 48, and 120 hpf embryos and cloned into pBluescript (BamHI-XhoI). Sequences of PCR primer pairs for the *cntnap2a* and

cntnap2b probes are:
***cntnap2a*, 520 bp:** 5' GCATAATCCACAACCTTCCAGTC 3' /
5' TTCCCCTGGTGCGAGACGGACAC 3'
***cntnap2b*, 1108 bp:** 5' GTGCTGGCAGCGGATTTTGGTG 3' /
5' CCTCCACCCCTCCAGGCATGAGC 3'

In addition, a second probe (517 bp) located closer to the 3' end of *cntnap2b* was found to have the same expression pattern as the longer probe (data not shown). Primers for this probe are:
5' CGAGTCTGCGGTGCTGGGCATTGTG 3' /
5' GACTCCCTGTATGGAGGCAGTGGAC 3'

Plasmids for transcribing the *in situ* probes for *gad1b, vglut2a, glyt2,* and *neurod1* were gifts from Brent Bill from the laboratory of Daniel Geschwind. The primer pairs for generating these probes are:

gad1b: 5' CGTCTTCTGCACCTTCTTCCT 3' /
5' AGATGTGAACAGCACGAGCC 3'
vglut2a: 5' AGGGAGCCTGCTGGTTTTAG 3' /
5' CTGCAGGTCCTAGCAGCTTAG 3'
glyt2: 5' TTGTGACGTGTACGAACAGC 3' /
5' CAAGTGGGTCGATCATGTTCT 3'
neurod1: 5' GCAGGATGCCTCCAACTGA 3' /
5' GTGACCGCAACGTAGAAGC 3'

The plasmid for transcribing *tag1* was a gift from the laboratory of Gavin Wright (Thisse et al., 2008), and *th1* was a gift from the laboratory of Pertti Panula (Chen et al., 2009).

Antisense digoxigenin (DIG)-labeled RNA probes were synthesized for 3 hours at 37°C in 20 µl reactions containing the following: 2 µl 10X transcription buffer (Roche), 2 µl 10X DIG RNA labeling mix (Roche), 1 µl 100 mM DTT (Roche), 1 µl RNaseOUT recombinant ribonuclease inhibitor (Invitrogen), 2 µl RNA polymerase (T7, SP6, or T3) (Roche), and 12 µl of linearized purified plasmid. Following probe synthesis, 2 µl of DNase I (amplification grade) (Invitrogen) was added to each sample for 30 minutes at 37°C. Probes were purified using the RNeasy Mini Kit (Qiagen). 24-48 hpf embryos were fixed in 4% paraformaldehyde (PFA) overnight at 4°C, washed in PBST (PBS + 0.1% Tween 20), dehydrated sequentially in methanol/PBST, and stored at -20°C at least overnight.

Immunohistochemistry

Whole mount antibody staining of dissected embryos was performed as previously described, with some modifications (Wilson et al., 1990). In brief, embryos were fixed in 4% sucrose/4% PFA at room temperature for 1 h per 24 h of development. Following fixation, embryos were washed in PBS and dissected according to the method previously described (Wilson et al., 1990), then dehydrated sequentially in methanol-PBT (PBS + 0.5% Triton X-100) and stored in methanol at -20°C at least overnight. Embryos were rehydrated sequentially, washed in PBT, digested with proteinase K (10 µg/ml for 10 minutes (28 hpf) or 20 minutes (48 hpf); 20-40 µg/ml for 72, 96, and 120 hpf, respectively for 20 minutes), and post-fixed in 4% sucrose/4% PFA for 20 minutes at room temperature. Embryos were blocked for at least 1 h at room temperature in 10% normal goat serum/1% DMSO/0.5% Triton X-100 in PBS, and incubated in primary antibodies overnight at 4°C. Embryos were washed 4-6 times for at least 30 minutes in PBT at room temperature and incubated in secondary antibodies for 2 h at room temperature or overnight at 4°C. Embryos were washed 4-6 times for at least 30 minutes at room temperature or overnight at 4°C in PBT and mounted for imaging in low melt agarose (0.8-1%). Tubes containing embryos were rotated at each step. Immunostaining to visualize forebrain commissure formation (Figure S1K-K') was performed in undissected embryos according to the method previously described (Barresi et al., 2005). The following primary antibodies were used: acetylated-Tubulin (mouse monoclonal IgG2b, #T7451, Sigma-Aldrich, RRID:AB_609894, 1:500 or 1:800); SV2 (mouse monoclonal IgG1, DSHB, 1:500); GABA (rabbit polyclonal, #A2052, Sigma-Aldrich,

RRID:AB_477652, 1:500); GFP (rat monoclonal IgG2a, #04404-84, Nacalai Tesque, Inc., RRID:AB_10013361, 1:1000); RFP (rabbit polyclonal, #600-401-379, Rockland, RRID:AB_2209751, 1:1000); GFAP (rabbit polyclonal, #Z0334, DAKO, RRID:AB_10013382, 1:400); Phospho-Histone H3 (Ser10) (rabbit polyclonal, #9701, Cell Signaling, RRID:AB_331535, 1:200). The following Alexa Flour secondary antibodies were used (Life Technologies, 1:200): 488 or 633 goat anti-mouse IgG2b; 568 goat anti-mouse IgG1; 488 or 546 goat anti-rabbit IgG (H+L); 488 goat anti-rat IgG (H+L).

TUNEL

TUNEL labeling to detect apoptotic cells was performed using the ApopTag kit (Chemicon International) with modifications to the standard protocol. 28 hpf embryos (undissected) were fixed in 4% PFA overnight at 4°C, washed in PBST (PBS + 0.1% Tween 20), sequentially dehydrated in methanol-PBST, and stored in methanol at -20°C at least overnight. Embryos were sequentially rehydrated and washed in PBST, then digested with proteinase K (10 µg/ml) for 18 minutes at room temperature and re-fixed in 4% PFA for 20 minutes at room temperature. Next, embryos were washed in PBST and incubated for 10 minutes in 2:1 ethanol:acetone at -20°C, washed again and incubated in equilibration buffer for 1 hour at room temperature. Embryos were rotated during all room temperature incubations. The following ratio of ApopTag enzyme and buffer was used: 12 µl TdT enzyme, 24 µl reaction buffer, and 1 µl of 10% Triton X-100. 18 µl of the reaction mix was added per tube containing 5-10 embryos overnight at 37°C. After the labeling reaction, embryos were washed in PBST, blocked, and developed as in the *in situ* hybridization protocol (Xu et al., 1994).

Imaging and data processing

Whole-mount immunostained embryos were imaged by confocal microscopy (Leica and Zeiss Systems, Yale Center for Cellular and Molecular Imaging; Leica Systems, UCL Research Department of Cell and Developmental Biology). Maximum intensity projections are shown for all confocal images, which were processed using Fiji (Schindelin et al., 2012), Imaris (Bitplane), or Volocity (Improvision). Dissected 24 hpf embryos were mounted laterally and imaged at 25X (0.8W) (Z-distance ≈ 74 µm). Dissected 48-120 hpf embryos were mounted at various orientations and imaged at 25X (0.95W) using Z-stacks ranging from ~150-250 µm. Embryos stained by fluorescent *in situ* hybridization were analyzed at 20X (0.8W) or 25X (0.95W). Figures were assembled using Illustrator (CC, Adobe).

To quantify GABA+ neurons at 28 hpf, dissected embryos were mounted laterally and imaged at 25X (0.8W). Z-stacks (80-110 µm, average=93 µm) started at the first appearance of the telencephalic neuropil and ended immediately past the midline at the point where GABA+ cells could no longer be visualized. Three blinded raters performed GABA cell counts on Z-stack images using the Cell Counter plug-in for Fiji (http://rsb.info.nih.gov/ij/plugins/cell-counter.html). This plug-in allows raters to manually mark individual cells in a z-stack and counts the cells as they marked. To quantify *dlx5a/6a:*GFP+ neurons in the forebrains of Tg(*dlx6a-1.4kbdlx5a/dlx6a:GFP*) larvae at 96 hpf, with or without early exposure to biochanin A (0.1 µM), dissected embryos were mounted laterally or ventrally and imaged at 25X (0.95W). Z-stacks (WT: lateral=300-340µm, average=323µm; ventral=250-290µm, average=273µm; *cntnap2ab*: lateral=260-330µm, average=302µm; ventral=240-300µm, average=267µm) were obtained of the whole brain, beginning and ending with the first and last appearance of the axon scaffold, respectively. *dlx5a/6a:*GFP+ neurons were counted in the forebrains of wild-type and mutant larvae in lateral and ventral images manually and blindly by a single rater using the Cell Counter plug-in for Fiji.

To measure head size, lateral images of live 30 hpf embryos or 96 hpf larvae anesthetized with MS-222 were obtained using a dissecting microscope. A single blinded rater traced the perimeter of the head using the otic vesicle as a posterior boundary, eye, and yolk using Fiji (Figures S1N-O and S1N'-O'). To measure brain size, maximum intensity projections of lateral and ventral confocal Z-stacks (WT: lateral=300-340µm, average=318µm; ventral=250-280µm, average=271µm; *cntnap2ab*: lateral=270-330µm, average=297µm; ventral=240-300µm, average=265 µm) of 96 hpf dissected whole brains stained with anti-acetylated tubulin were imaged at 25X (0.95W). Using Fiji, a single blinded rater traced the perimeter of the brain with the midbrain-hindbrain boundary as

the posterior boundary (Figures S1P-Q and S1P'-Q').

To analyze forebrain commissure formation, embryos were cleared in 75% glycerol, mounted between two cover slips, and imaged at 40X (1.2W) in Z-stacks of ~14 μm. Three blinded raters assessed the degree of forebrain commissure formation in maximum intensity projection images based on a previously defined scale (Barresi et al., 2005). Whole mount *in situ* images were analyzed using Zeiss Axioimager M1 and Discovery microscopes and photographed with a Zeiss Axiocam digital camera. Images were processed with Zeiss AxioVision 3.0.6.

Imaris 7.7.2 software (Bitplane) was used to quantify *dlx5a/6a:*GFP+ neurons and *vglut:*DsRed and acetylated tubulin surface area by brain region in Tg(*dlx6a-1.4kbdlx5a/dlx6a:GFP*::*vglut:DsRed*) larvae at 4 dpf. First, a surface was generated to demarcate each region. To quantify markers in lateral images, the surface was traced from the lateral edge to the mid-line of the brain, which demarcated the region where the staining was strongest. The following mounting orientations were used to quantify the respective regions: forebrain and hypothalamus: ventral and lateral; optic tectum and cerebellum: dorsal and lateral. *dlx5a/6a:*GFP+ cells were counted using an estimated XY diameter = 6 μm and filtered by quality with the following cutoffs: forebrain and hypothalamus, 23; cerebellum, 15; optic tectum, 10. *vglut:*DsRed and acetylated tubulin surface area were measured using a surface area detail level = 1.000 μm and the smooth function with the following absolute intensity cutoffs for glutamate (*vglut*) and tubulin (AcTub): forebrain: *vglut,* 40 and AcTub, 25; hypothalamus: *vglut*, 40 (ventral images)/30 (lateral images) and AcTub, 25; cerebellum: *vglut,* 30 (dorsal images)/25 (lateral images) and AcTub, 25; optic tectum, *vglut,* 25 and AcTub, 15. Cell number and surface area values were normalized to the wild-type average for each orientation. Images were analyzed blindly by a single rater. Statistical analyses were conducted using StatPlus (AnalystSoft).

RT-PCR

Total RNA was extracted from 25 wild-type, *cntnap2a*$^{\Delta 121/\Delta 121}$*cntnap2b*$^{31i/31i}$ or *cntnap2a*$^{\Delta 121/\Delta 25}$*cntnap2b*$^{31i/\Delta 7}$ larvae at 5 dpf using TRIzol reagent (Life Technologies) and purified using the RNeasy Mini Kit (Qiagen). First strand cDNA synthesis was performed according to the manufacturer's recommendations using SuperScript II or III First-Strand Synthesis System (Invitrogen). Limited-cycle PCR to amplify exons 1 to 6 of *cntnap2a* and *cntnap2b*, which is the region containing ZFN-induced indel mutations, was performed using the following primer pairs:

***cntnap2a*, 808 bp:** 5' ATTTTAAGCCACATCAGCATCTCTC 3' /
5' TTCTCCTGTAGCGCTCAATTACTAC 3'

***cntnap2b*, 718 bp:** 5' TATGGTGTGTTTATGTGAAGCTCAG 3' /
5' TGAATGGAGCCGTACTGATTACT 3'

Genomic DNA lengths for these primer pairs are: *cntnap2a:* 356,671 bp; *cntnap2b:* 40,857 bp. Sanger-sequencing of *cntnap2a* and *cntnap2b* RT-PCR products from wild-type cDNA produced clear sequences with no evidence of exon-skipping involving exons 1-6. Sanger sequencing of RT-PCR products from cDNA from *cntnap2a*$^{\Delta 121/\Delta 25}$*cntnap2b*$^{31i/\Delta 7}$ transheterozygotes indicated that both mutant alleles were being transcribed. To resolve the sequences of these transcripts and to assess for alternatively spliced transcripts in this region in *cntnap2a*$^{\Delta 121/\Delta 121}$*cntnap2b*$^{31i/31i}$ and *cntnap2a*$^{\Delta 121/\Delta 25}$*cntnap2b*$^{31i/\Delta 7}$ larvae, RT-PCR products from these mutants were cloned using either TOPO-TA or Zero Blunt PCR TOPO Cloning Kit (Invitrogen) and plasmid DNA was isolated (QIAprep Miniprep kit, Qiagen) from ~10 colonies per PCR product and Sanger-sequenced (Keck Biotechnology Resource Laboratory, Yale University).

Generation of antibodies against zebrafish Cntnap2a and Cntnap2b

Custom antibody recognizing zebrafish Cntnap2a and Cntnap2b (YZ3970) was generated by YenZym Antibodies, LLC, using a peptide antigen corresponding to amino acids 867 to 886 of Cntnap2a: TPLNDDQWHRVSAERNTKEAC-amide. This region is 90% identical between Cntnap2a and Cntnap2b and occurs within the third Laminin-G domain of both proteins. To verify that this antibody recognized both Cntnap2 proteins, HA-tagged full-length Cntnap2a and Cntnap2b were cloned into pCS2+ and transfected into HEK cells using lipofectamine 2000 reagent (Invitrogen). Total protein was isolated from transfected HEK cells and analyzed

by SDS-PAGE and western blotting. YZ3970 was found to recognize both overexpressed proteins by western blot (data not shown).

Western blot

To analyze Cntnap2a and Cntnap2b expression, total protein was isolated from the heads of 72 hpf larvae with the following genotypes: wild-type, *cntnap2ab* double homozygotes, single homozygotes, and double heterozygotes from both mutant lines (*cntnap2a*$^{\Delta 121/\Delta 121}$*cntnap2b*$^{31i/31i}$ and *cntnap2a*$^{\Delta 25/\Delta 25}$*cntnap2b*$^{\Delta 7/\Delta 7}$). 10 ml of lysis buffer was prepared fresh containing 1 ml of 10X Cell Lysis Buffer (#9803, Cell Signaling), 100 µl of 0.1 M PMSF, 1 complete protease inhibitor cocktail tablet (Roche), and 9 ml distilled water. Protein was isolated using 150 µl of lysis buffer per 62 decapitated 72 hpf heads. Samples were homogenized on ice by mechanical grinding, then rotated at 4°C for 20 minutes and immediately stored at -80°C at least overnight. Upon thawing, samples were centrifuged at 13,000 rpm for 3 minutes to pellet insoluble material. 20 µl of the supernatant from each sample was diluted 1:1 in 2X loading buffer (prepared from 4X NuPAGE LDS Sample Buffer, Invitrogen) with 20% β-mercaptoethanol, and boiled for 2 minutes at 95°C. 30-34 µl of each sample was loaded per lane and analyzed by SDS-PAGE using 7.5% mini-PROTEAN TGX precast gels (Bio-Rad). The polyacrylamide gel was transferred to a PVDF membrane using a wet transfer system (Bio-Rad). Primary antibodies used for western blotting included: Affinity-purified custom antibody directed against Cntnap2A and Cntnap2B (YenZym, YZ3970, 1:500); β-actin (mouse monoclonal, #A1978, Sigma-Aldrich, RRID:AB_476692, 1:5000). After probing with primary antibody, blots were stripped with Restore Western Blot Stripping Buffer (Thermo Scientific) and reprobed with antibody to β-actin. Secondary antibodies included peroxidase-conjugated AffiniPure donkey anti-rabbit IgG (H+L) and peroxidase-conjugated AffiniPure donkey anti-mouse IgG (H+L) (Jackson ImmuoResearch Laboratories, Inc., 1:10:000).

Locomotor activity assay

The behavioral assay was conducted as described previously (Prober et al., 2006; Rihel et al., 2010). In brief, individual 4 dpf larvae were placed in a 96-well plate (7701-1651; Whatman, Clifton, NJ) containing 650 µl of standard embryo water (0.3 g/L Instant Ocean, 1 mg/L methylene blue, pH 7.0). The 96-well plate was maintained at a constant temperature (28.5°C) and exposed to a 14h:10h white light:dark schedule with constant infrared illumination within a custom-modified Zebrabox (Viewpoint, LifeSciences) (Figure 2A). Larval activity was monitored for 60-72 hours using an automated video tracking system (Zebrabox and Videotrack software; Viewpoint Life Sciences, Montreal, Quebec, Canada). Larval movement was recorded using Videotrack quantization mode. The Videotrack detection parameters were empirically defined for clean detection of larval movement with minimal noise. To control for differences in genetic background, all tracking experiments were performed blindly on the progeny of double heterozygous *cntnap2a*$^{+/-}$*2b*$^{+/-}$ fish. After tracking, genomic DNA was isolated from individual larvae and genotyping was done by PCR and high-resolution fragment analysis (DNA Analysis Facility at Yale University).

Pentylenetetrazol activity assay

For the dose-response experiments, individual *cntnap2a*$^{\Delta 121/\Delta 121}$*cntnap2b*$^{31i/31i}$ or wild-type larvae at 4 or 6 dpf were pipetted into the wells of a 96-well plate containing 650 µl of standard embryo water. As above, the plate was placed in a custom-modified Zebrabox. Larval movement was recorded by the Videotrack system for 1 h before and after the addition of PTZ or water. Videotrack detection parameters were determined as above. PTZ was diluted in sterile distilled water and either PTZ or water alone was pipetted directly into each well to yield the following PTZ final concentrations: 2.5, 5, 7.5, 10, and 15 mM. At 6 dpf, the total number of larvae tested per concentration of PTZ was: 2.5, 5, 7.5, 10 mM, n=42-48; 15 mM, n=24; water only, n=68. At 4 dpf: 2.5, 7.5, 15 mM, n=10-12; 5, 10 mM, water only, n=34. Data were analyzed by normalizing the post-PTZ activity of each fish to itself prior to the addition of PTZ or water. For blinded experiments, the progeny of incrosses of *cntnap2a*$^{\Delta 25/+}$*cntnap2b*$^{\Delta 7/+}$ fish at 4 dpf (n=268) were pipetted individually into the wells of a 96-well plate. Sterile water or PTZ (final concentration=10 mM) was pipetted directly into the wells of one-half of the same 96-well plate. 10 mM PTZ was

selected because this dose was found to illicit the largest differential response in wild-type versus mutant fish at 6 dpf (Figure S3C). Genomic DNA isolation and genotyping were performed after each experiment.

Chemical screens

Selection of psychoactive agents was based on the following criteria (Figure 3A): i) behavioral phenotype of wild-type fish plus drug strongly correlates with the phenotype of *cntnap2a*$^{\Delta 25/\Delta 25}$*cntnap2b*$^{\Delta 7/\Delta 7}$ mutants (L-701,324 and MK-801); ii) behavioral phenotype of wild-type fish plus drug strongly anti-correlates with the mutant phenotype (9 drugs); iii) GABAergic mechanism (zolpidem, diazepam); iv) clinical use in treating aggression or irritability in ASD (risperidone). Three doses of each drug were selected based on previous studies of the dose range that induces behavioral effects and minimizes toxicity in larval zebrafish (Rihel et al., 2010). All agents were dissolved in DMSO with the exception of baclofen, which was dissolved in water. DMSO alone at <0.2% has been shown not to affect behavior (Rihel et al., 2010). Each drug concentration was tested on 10-12 *cntnap2a*$^{\Delta 121/\Delta 121}$*cntnap2b*$^{31i/31i}$ or wild-type larvae, with 10-12 control larvae per 96-well plate. Stock solutions of each compound dissolved in DMSO or DMSO alone were pipetted directly into the wells of a 96-well plate containing 650 µL of standard embryo water.

Final concentrations of each drug tested in wild-type and *cntnap2a*$^{\Delta 121/\Delta 121}$*cntnap2b*$^{31i/31i}$ larvae are shown in Table S4. Amantadine was identified as anti-correlating by using a more extensive dataset of 6,000 compounds, which was previously filtered to yield the list of 550 compounds (Rihel et al., 2010). For blinded experiments, the progeny of incrosses of *cntnap2a*$^{\Delta 25/+}$*cntnap2b*$^{\Delta 7/+}$ fish (n=560, 2 independent experiments) were pipetted individually into the wells of a 96-well plate. DMSO or biochanin A (final concentration=0.1-1µM) was pipetted directly into the wells of one-half of the same 96-well plate. Genomic DNA was isolated and fish were genotyped after each experiment.

Hierarchical clustering

Behavioral phenotypes of wild-type fish exposed to a panel of 550 psychoactive agents from 4 to 7 dpf were ascertained as previously described (Rihel et al., 2010). To compare the behavioral fingerprints of wild-type larvae exposed to each drug and the *cntnap2a*$^{\Delta 25/\Delta 25}$*cntnap2b*$^{\Delta 7/\Delta 7}$ mutant behavioral fingerprint, hierarchical clustering analysis was performed as in (Rihel et al., 2010).

Correlation analysis

Correlation analysis was performed in Matlab (R2014a; The Mathworks, Inc.) as previously described (Rihel et al., 2010).

Rank correlation analysis

To conduct rank correlation analysis of NMDA antagonists and estrogenic analogs, compounds were assigned to pharmacological classes as described (Rihel et al., 2010). Estrogenic agents were additionally annotated by hand blind to rank using PubChem (pubchem.ncbi.nlm.nih.gov/). Assays of bioactivity in a set of *in vitro* estrogen receptor-α tests deposited at PubChem were included. Insecticides were the only class of compounds that were excluded due to their strong effects on sodium channels. Rank correlation analysis was performed as described using the Kolmogorov-Smirnov statistic to assess significance (Rihel et al., 2010). Rank-sorting of anti-correlating drugs revealed that estrogenic compounds are significantly enriched in this dataset. Specifically, 25 compounds in our dataset of 550 were identified as estrogenic. Four of the top 10 anti-correlating agents are estrogenic. We created 10,000 randomly permuted datasets and found similar or better enrichment in only three permuted datasets, giving a p-value estimate of 3/10,000 or 0.0003. Using both strict and relaxed criteria for defining estrogenic agents demonstrated enrichment of these agents in the top ranks.

Principal components analysis

Data were aggregated for 18 rest-wake parameters (sleep, rest bouts, average total activity, average waking activity; each of these parameters was determined for nights 5 and 6 and days 5 and 6; and night and day average

waking activity) and each drug-dose combination. For the differential response PCA, each data point was defined as the Z-score of the response of wild-type or *cntnap2a*$^{\Delta 12 1/\Delta 12 1}$*cntnap2b*$^{31i/31i}$ mutant larvae to each drug compared to their baseline (DMSO alone). For the PCA to identify drugs that reverse the behavioral fingerprint of mutants, each data point was defined as the Z-score of the response of *cntnap2a*$^{\Delta 12 1/\Delta 12 1}$*cntnap2b*$^{31i/31i}$ mutant larvae exposed to each drug compared to the behavioral fingerprint of untreated wild-type larvae. Hierarchical clustering was conducted in Matlab (R2014a), with the statistics and bioinformatics toolboxes. PCA was performed according the method described in (Woods et al., 2014).

Long-term Exposure to Biochanin A

To assess the extent to which exposure to biochanin A affects GABAergic cell numbers, biochanin A dissolved in DMSO or DMSO alone was added to petri dishes containing Tg(*dlx6a-1.4kbdlx5a/dlx6a:GFP*) wild-type or *cntnap2a*$^{\Delta 12 1/\Delta 12 1}$*cntnap2b*$^{31i/31i}$ embryos at 30 hpf (n=6-11/dish) and embryos were raised in the presence of either biochanin A (final concentration=0.1 μM) or DMSO. At 4 dpf, larvae were fixed, dissected, immunostained and imaged by confocal microscopy, as described above. *dlx5a/6a:*GFP+ cells in the forebrain were counted manually as described.

To determine the extent to which chronic exposure to biochanin A affects nighttime hyperactivity, wild-type or *cntnap2a*$^{\Delta 12 1/\Delta 12 1}$*cntnap2b*$^{31i/31i}$ embryos were exposed to biochanin A (1 μM) dissolved in DMSO or DMSO alone at 24 hpf (n=50/dish). Biochanin A (1 μM) or DMSO was added daily. At 4 dpf, each larva was pipetted into fresh embryo water, allowed to swim for 30 seconds, and placed in a 96-well plate with fresh embryo water. The locomotor activity of wild-type or mutant embryos was tracked for 48 hours using the automated tracking assay described above.

To test the effect of biochanin A exposure on PTZ-induced seizures, wild-type or *cntnap2a*$^{\Delta 12 1/\Delta 12 1}$*cntnap2b*$^{31i/31i}$ embryos were exposed to biochanin A (1 μM) dissolved in DMSO or DMSO alone at 24 hpf (n=50/dish) and biochanin A (1 μM) or DMSO was added daily. At 4 dpf, larvae were plated in a 96-well plate containing either biochanin A or DMSO. Larvae were allowed to habituate for 15 minutes and baseline locomotor activity was tracked for two hours, after which 10 mM PTZ was added to each well and locomotor activity was tracked for two hours using the automated assay described above.

qPCR

To assess the effect of biochanin A exposure on estrogen target genes, groups of ~35 wild-type larvae were exposed to biochanin A (1 μM, 10 μM) or DMSO overnight from 4 to 5 dpf. Biochanin A (1 μM, 10 μM) and DMSO exposure were conducted in duplicate samples. Total RNA was isolated using TRIzol reagent (Life Technologies) and purified using the RNeasy Mini Kit (Qiagen). cDNA was synthesized using 1000 ng of total RNA and the SuperScript III First-Strand Synthesis System (Invitrogen). Expression of the following three genes was analyzed by qPCR: *vitellogenin 1* (*vtg1*); *estrogen receptor 1* (*esr1*); *cytochrome P450, family 19, subfamily A, polypeptide 1* (*aromatase B, cyp19a1b*). These genes were selected because they were found to be upregulated in response to 17β-estradiol in zebrafish embryos (Hao et al., 2013). We selected *cyp19a1b* because it is expressed in the brain during early development (Hao et al., 2013). *cyp19a1b* primer sequences were obtained from (Hao et al., 2013). Primer sequences for *vtg1* and *esr1* are shown below:

***vtg1*, 106 bp:** 5’ GAGATGCAAGAGGCTGGAG 3’ /
5’ GGCTCAGATCTTTAGACTTTGTCAC 3’
***esr1*, 122 bp:** 5’ TTACGGAGTCTGGTCGTGTG 3’ /
5’ AGCTCTTTCGACGGTTTCTG 3’

Other larval behavioral assays

Acoustic startle, habituation, and PPI were analyzed in *cntnap2a*$^{\Delta 12 1/\Delta 12 1}$*cntnap2b*$^{31i/31i}$ (n≈70), *cntnap2a*$^{\Delta 12 1/+}$*cntnap2b*$^{31/+}$ (n≈70), and wild-type (n≈50) larvae at 5 to 7 dpf by raters blind to genotype, according to the method previously described (Wolman et al., 2011). After the initial analysis indicated that there may be a difference in the LLC response rate of mutants, the progeny of incrosses of *cntnap2a*$^{\Delta 12 1/+}$*cntnap2b*$^{31i/+}$ fish were

blindly tested for LLC responsiveness and genotyped after the experiment (total n=318; *cntnap2a*$^{\Delta 12l/\Delta 12l}$*cntnap2b*$^{31i/31i}$, n=14; *cntnap2a*$^{\Delta 12l/+}$*cntnap2b*$^{31i/+}$, n=92; wild-type, n=24). The optokinetic response assay was performed on *cntnap2a*$^{\Delta 12l/\Delta 12l}$*cntnap2b*$^{31i/31i}$ (n=18), *cntnap2a*$^{\Delta 12l/+}$*cntnap2b*$^{31/+}$ (n=11), and wild-type (n=14) larvae at 5 to 7 dpf with different contrast levels of the visual stimulus (5-100%). Two independent trials were conducted by raters blind to genotype, according to the previously described method (Schoonheim et al., 2010).

Supplemental References

Barresi, M.J., Hutson, L.D., Chien, C.B., and Karlstrom, R.O. (2005). Hedgehog regulated Slit expression determines commissure and glial cell position in the zebrafish forebrain. Development *132*, 3643-3656.

Burgess, H.A., and Granato, M. (2007). Sensorimotor gating in larval zebrafish. The Journal of neuroscience *27*, 4984-4994.

Chen, Y.C., Priyadarshini, M., and Panula, P. (2009). Complementary developmental expression of the two tyrosine hydroxylase transcripts in zebrafish. Histochemistry and cell biology *132*, 375-381.

Cifuentes, D., Xue, H., Taylor, D.W., Patnode, H., Mishima, Y., Cheloufi, S., Ma, E., Mane, S., Hannon, G.J., Lawson, N.D*., et al.* (2010). A novel miRNA processing pathway independent of Dicer requires Argonaute2 catalytic activity. Science *328*, 1694-1698.

Doyon, Y., McCammon, J.M., Miller, J.C., Faraji, F., Ngo, C., Katibah, G.E., Amora, R., Hocking, T.D., Zhang, L., Rebar, E.J*., et al.* (2008). Heritable targeted gene disruption in zebrafish using designed zinc-finger nucleases. Nature biotechnology *26*, 702-708.

Foley, J.E., Maeder, M.L., Pearlberg, J., Joung, J.K., Peterson, R.T., and Yeh, J.R. (2009). Targeted mutagenesis in zebrafish using customized zinc-finger nucleases. Nature protocols *4*, 1855-1867.

Hao, R., Bondesson, M., Singh, A.V., Riu, A., McCollum, C.W., Knudsen, T.B., Gorelick, D.A., and Gustafsson, J.A. (2013). Identification of estrogen target genes during zebrafish embryonic development through transcriptomic analysis. PloS one *8*, e79020.

Julich, D., Hwee Lim, C., Round, J., Nicolaije, C., Schroeder, J., Davies, A., Geisler, R., Lewis, J., Jiang, Y.J., Holley, S.A*., et al.* (2005). beamter/deltaC and the role of Notch ligands in the zebrafish somite segmentation, hindbrain neurogenesis and hypochord differentiation. Developmental biology *286*, 391-404.

Miller, J.C., Holmes, M.C., Wang, J., Guschin, D.Y., Lee, Y.L., Rupniewski, I., Beausejour, C.M., Waite, A.J., Wang, N.S., Kim, K.A*., et al.* (2007). An improved zinc-finger nuclease architecture for highly specific genome editing. Nature biotechnology *25*, 778-785.

Sander, J.D., Dahlborg, E.J., Goodwin, M.J., Cade, L., Zhang, F., Cifuentes, D., Curtin, S.J., Blackburn, J.S., Thibodeau-Beganny, S., Qi, Y*., et al.* (2011). Selection-free zinc-finger-nuclease engineering by context-dependent assembly (CoDA). Nature methods *8*, 67-69.

Schindelin, J., Arganda-Carreras, I., Frise, E., Kaynig, V., Longair, M., Pietzsch, T., Preibisch, S., Rueden, C., Saalfeld, S., Schmid, B*., et al.* (2012). Fiji: an open-source platform for biological-image analysis. Nature methods *9*, 676-682.

Schoonheim, P.J., Arrenberg, A.B., Del Bene, F., and Baier, H. (2010). Optogenetic localization and genetic perturbation of saccade-generating neurons in zebrafish. The Journal of neuroscience *30*, 7111-7120.

Thisse, B., Wright, G.J., and Thisse, C. (2008). Embryonic and Larval Expression Patterns from a Large Scale Screening for Novel Low Affinity Extracellular Protein Interactions.

Thisse, C., Thisse, B., Schilling, T.F., and Postlethwait, J.H. (1993). Structure of the zebrafish snail1 gene and its expression in wild-type, spadetail and no tail mutant embryos. Development *119*, 1203-1215.

Wilson, S.W., Ross, L.S., Parrett, T., and Easter, S.S., Jr. (1990). The development of a simple scaffold of axon tracts in the brain of the embryonic zebrafish, Brachydanio rerio. Development *108*, 121-145.

Wolman, M.A., Jain, R.A., Liss, L., and Granato, M. (2011). Chemical modulation of memory formation in larval zebrafish. Proceedings of the National Academy of Sciences of the United States of America *108*, 15468-15473.

Woods, I.G., Schoppik, D., Shi, V.J., Zimmerman, S., Coleman, H.A., Greenwood, J., Soucy, E.R., and Schier, A.F. (2014). Neuropeptidergic signaling partitions arousal behaviors in zebrafish. The Journal of neuroscience *34*, 3142-3160.

Xu, Q., Holder, N., Patient, R., and Wilson, S.W. (1994). Spatially regulated expression of three receptor tyrosine kinase genes during gastrulation in the zebrafish. Development *120*, 287-299.